Nanofibrous composite meshes for surgical tissue regeneration

Thesis Booklet

Constantinos Voniatis MD

Semmelweis University
Doctoral School for Theoretical and Translational Medicine

Supervisors:
Dr. Angéla Jedlovszky-Hajdú, PhD., Associate Professor
Dr. Andrea Ferencz MD, PhD., Associate Professor

Official reviewers:
Romána Zelkó, PhD., D.Sc, Professor
György Marosi, PhD., D.Sc, Professor

Head of the Examination Committee:
Zoltán Benyó, M.D., PhD., D.Sc., Professor

Members of the Examination Committee:
László Mátyus, PhD., D.Sc., Professor
László Harsányi, PhD., D.Sc, Professor
András Deák, MSc, PhD. Associate Profesor

Budapest
2022

1. Introduction

Compared to its early days, medicine is exceedingly advanced and together with the evolution of the civilised world had two intertwined effects: increasing the average life expectancy and increasing the incidence of long-term complications of chronic diseases and disorders.

Often perceived as medicine's ultimate goal, regeneration of tissues is a highly challenging, strenuous, and complex task. Various approaches, methods, and tactics are being researched and implemented. Amongst them, tissue engineering and the development of tissue scaffolds i.e., tissue templates resembling the extracellular matrix has perhaps the greatest and most promising potential. A globally accepted effective and promising approach, is the fabrication of polymer-based membranes, meshes or mats composed nano-sized fibres.

These materials have a microstructure that resembles the body's innate extracellular matrix, a paramount structure found around almost every human cell and tissue responsible for cell adhesion, proliferation and even cell signalling . After implanting such membranes, native cells in the patient's body can adhere,
proliferate, and even differentiate on them making them therefore excellent tissue scaffolds. However, as any material intended for medical and biomedical applications these membranes have serious prerequisites and criteria to fulfil.

Fabrication of polymer-based membranes or meshes can be achieved utilising electrospinning. While having innumerable options and modifications, electrospinning in its most basic form is the formation of fibres from polymer

solutions via using an electrostatic force gained by a power supply.

In this work polysuccinimide (PSI) was chosen as the primary component as it can be regarded as a promising candidate for surgical tissue regeneration as being an amino acid derivative (under physiological conditions it turns to poly(aspartic acid) (PASP)), fabricated meshes should be biocompatible and biodegradable.

2. Objectives

The aim of the thesis can be shortly summarised for four frames:

A. Optimisation of PSI electrospun membranes for different biomedical applications.

B. Fabrication, characterisation and investigation of the *in vitro*/*in vivo* behaviour of co-electrospun polysuccinimide/poly(vinyl alcohol) meshes.

C. Fabrication and characterisation and investigation of the in vitro/in vivo behaviour of layered-, co-, and blend-electrospun polysuccinimide/polycaprolactone meshes.

D. Functionalisation of PSI and PSI composite electrospun meshes with magnetite nanoparticles for MRI tracing.

One important aspect of this work was to attempt and include the entire biomaterial development process including synthesis and fabrication, and the characterisation of parameters

(chemical, physical, mechanical, biological) relevant to surgical tissue regeneration.

3. Materials and Methods

3.1 Synthesis of Polysuccinimide

L-aspartic acid and phosphoric acid were mixed at a 1:1 mass ratio and mixed in a rotary vacuum evaporator system. The mixture was heated to 180 °C while the pressure inside the flask was decreased to 5 mbar at a predetermined gradual rate. The entire synthesis lasted 8 hours. Subsequently, PSI was then dissolved in DMF, precipitated and thoroughly washed in ultrapure water until the supernatant became neutral then dehydrated in a dehydration chamber.

3.2 PSI solubility, conductivity and viscosity studies

To investigate PSI solubility, solvents typically used for electrospinning were examined. Subsequently, viscosity and conductivity of the polymer solutions. Viscosity studies were performed with a SV-10 Vibrational Viscometer (A&D Company, Limited, Japan) for the specific and a MFR 2100 Micro Fourier Rheometer (GBC Scientific Equipment Pty Ltd, Australia) for relative measurements. An Orion Star™ Series Meter (Thermo Fisher Scientific, USA) was then used for conductivity assessments.

3.2 Electrospinning

Polymer solutions were prepared with ultrapure water for PVA (15w/w %), DMF for PSI (25w/w %), and DMF/THF for PCL (15w/w %). For fabricating single component meshes (PSI, PCL, PVA) a conventional electrospinning setup with a

rotating cylindrical collector was used. For layer-electrospinning two different polymer solution were electrospun one after the other on the same collector. Co-electrospinning was produced by concurrently electrospinning two different polymer solutions (PSI and PCL or PSI and PVA). Blend-electrospinning was executed by first mixing two polymer solutions (PSI and PCL) immediately before the electrospinning session.

3.3 Post-electrospinning processing

After electrospinning mechanical and chemical treatments were necessary. Specifically meshes were folded and compressed then chemically treated to create cross-links between the polymer chains. PSI cross-linking was achieved by immersion of PSI containing meshes (PSI, PSI/PVA,PSI/PCL) in 1,4-Diaminobutane (DAB). PVA containing meshes were immersed in 2M HCL to catalyse glutaraldehyde-based crosslinking (PVA, PSI/PVA).

3.4 Chemical and Physical Characterisation of PSI and PSI Composite Meshes

Chemical analysis of the electrospun fibrous meshes was performed using an FTIR spectrophotometer (4700 series type A, JASCO, Japan), equipped with a diamond ATR head (ATR Pro One, JASCO, Japan). To examine the fibre quality and size and morphology Scanning Electron Microscopy (JSM 6380LA, JEOL, Japan), two photon excitation microscopy (Femto2D series, Femtonics, Hungary) and fluorescence microscopy (Nikon Eclipse E600 Fluorescence Microscope, Nikon, Japan) was utilised. To examine the magnetite

nanoparticles Transmission Electron Microscopy (FEI Morgagni Transmission Electron Microscope) were used.

3.6 Wettability Studies

Assessment of wettability was performed on small circular samples from each mesh. Assessments were performed using a contact angle meter with a built-in camera (OCA 15 Plus, Dataphysics, Germany). Initial water angles (θ) were measured as well as absorption times (t) when applicable.

3.7 Mechanical Studies

To assess the mechanical parameters of the meshes, samples (1.5 cm x 6 cm) were taken from every mesh in both a vertical and horizontal orientation (to that of the collector's axis of rotation) direction. A uniaxial mechanical tester (4952, Instron, USA) was utilised. To be as comprehensive and objective as possible, the surface area and the mass of the samples were both taken into consideration. A specific loading capacity was calculated using the following formula:

$$\textbf{Specific Load Capacity}\ \left(\frac{\boldsymbol{N\,m^2}}{\boldsymbol{g}}\right) = \frac{Maximal\ Sustained\ Load\ (N)}{Area\ Density\ \left(\frac{g}{m^2}\right)}$$

where

$$\textbf{Area Density}\ \left(\frac{\boldsymbol{g}}{\boldsymbol{m^2}}\right) = \frac{Sample\ Mass\ (g)}{Sample\ Surface\ Area\ (m^2)}$$

Measurements were performed in air and under liquid

3.8 Cell Studies of PSI and PSI Composite Meshes

Cell viability, morphology and adhesion were examined with 155BR adherent human skin fibroblast cells

(ECACC 90011809) . Cell viability was examined after 24 and 72 hours by measuring the concentration of WST-1 reagant.

For observation of cell adhesion, disk shaped fibrous samples were sterilised then rinsed in cell culture medium twice the day before cell seeding. On the following day the disks were rinsed in a fresh cell culture medium for 2 hours. Cells were labelled with fluorescent vital dye Vybrant DiD before seeding onto the fibrous samples. were placed onto round glass coverslips in the wells. Wells containing cells seeded on glass coverslips were used as control. After 72 hours of seeding, samples were washed with tempered PBS (37 °C) then fixed with 4% para-formaldehyde (PFA) at room temperature for 20 min. Samples were stored at 4 °C until examination under a Femto2d two-photon microscope (Femtonics, Hungary). A Spectra Physics Deep See laser was used with 800 nm wavelength to induce the photoactive stain.

3.9 Biocompatibility Studies

In order to examine a biomaterials biocompatibility and biodegradability profile, *in vivo* animal experiments are required. For this purpose, Wistar rats were chosen as the animal model according to the European Union's 2010/63/EU and EU 2019/1010 directive on the protection of animals used for scientific purposes. Rats possess the size, blood volume, and easy handling properties required for the study.

Anaesthesia and analgesia were performed by intraperitoneal injection of a 4:1 Ketamine (70 mg/bodyweight kg) and Xylazine (10 mg/bodyweight kg). Before implantation, the samples were sterilized by immersion in a PBS/ClO_2 solution for 30 minutes. The surgical procedure was entirely aseptic. Two samples (1.5 x 1.5 cm) were implanted in every

animal After a dorsal median 5 – 6 cm incision on the back along the nuchal ligament the subcutaneous tissue was bluntly dissected to ensure enough space for the samples. Samples were fixated along the dorsal median line on the underlying fascia and muscle with a simple interrupted stich. Non-cross-linked samples were fixated cranially while cross-linked ones were always secured caudally. Skin closure was performed with an intracutaneous suture technique. For both fixation and skin closure an Atramat 4-0 polyglycolic acid absorbable suture material was used.

In the case of the PSI-DAB-Magn investigation only one sample (1x1 cm) was implanted in a similar manner to prevent sample interference issues during MRI examinations

4. Results

In this thesis electrospun nanofibrous meshes have been fabricated, optimised and examined as biomaterials intended for surgical tissue regeneration using different polymer sources. The main polymer used was polysuccinimide, the anhydrous form of a synthetic poly (amino acid) with a high functionalisation profile.

Throughout the work of this thesis, the following new scientific results have been achieved:

T1. Polysuccinimide meshes were successfully optimised in terms of fibre size and mechanical properties. The starting average fibre diameter measuring 615 ± 105 nm was reduced to 280 ± 50 nm via the optimisation of polymer concentration, needle size, flow rate and voltage. Mechanical enhancement

was also successful improving the specific loading capacity of the meshes uniaxially from 0.3 to 0.7 Nm2/g due to fibre alignment but also biaxially using the multilayer stacking technique. (I./III.)

T2. PSI was successfully combined with PVA to fabricate co-electrospun composite meshes, for the first time in current literature. ATR-FTIR proved the presence of the two polymer fibres in the samples while the two-photon excitation microscopy confirmed their random distribution along the sample surface (Figure 1.). The PVA component improved the mechanical performance of the meshes under liquid reaching a specific loading capacity of 0.164 Nm2/g. On the other hand, the PSI component increased wettability. Compared to pure PVA meshes which although hydrophilic did not let water pass through, PSI/PVA meshes evidently exhibited a definitive and measurable absorption time. (II.)

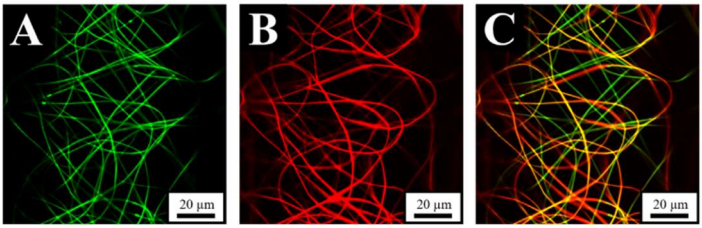

Figure 1. TPEM micrographs of co-electrospun PSI/PVA meshes: A. PSI fibres – low green channel, B.PVA fibres - low red channel C. PSI/PVA fibres both channels

T3. Biocompatibility of the co-electrospun PSI/PVA meshes was examined in vitro with a fibroblast cell line and in vivo on small animals, specifically Wistar rats. Meshes proved to be cyto, haemo- and biocompatible (Figure 2,3). As pure PVA and PSI/PVA meshes provided poor cell adhesion thus they can be described as antiadhesive. During the animal studies

macroscopical and microscopical biocompatibility was evident while enhanced tissue integration after 2 weeks is highly suggestive.

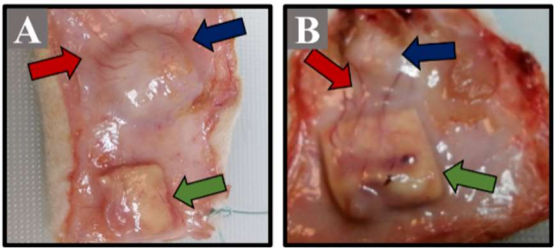

Figure 2. Macroscopical findings during sample retrieval: A. Co-spun PSI/PCL (blue arrow), Co-spun PSI-DAB/PCL (green arrow), B. Blend-spun PSI/PCL (blue arrow), Blend-spun PSI-DAB/PCL (green arrow), Newly formed vessels (neovascularisation is indicated with red arrows)

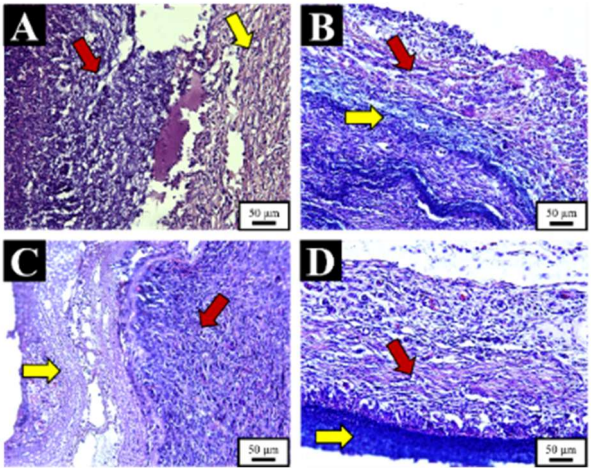

Figure 3. Figure 54. Histopathology examination of: A. PSI-DAB, B.PSI/PVA-GDA, C. PSI-DAB/PVA-GDA, D. PVA-GDA. Yellow Arrow: Implant, Red Arrow: Granulation Tissue

T4. Three different PSI/PCL composite meshes were successfully fabricated for the first time in current literature by utilising three different electrospinning configurations: layer-electrospinning, co-electrospinning and blend-electrospinning. While ATR-FTIR demonstrated no difference in the chemical composition of these composite meshes, fluoresce microscopy confirmed that in the case of co-electrospun meshes two different polymer fibres are present (PSI and PCL) while in the case of the blend-electrospun meshes both polymers are present within the electrospun fibres. In term of mechanical performance layer-electrospun meshes proved the strongest both in air and under liquid exhibiting a specific loading capacity of 0.455 ± 0.155 and 0.332 ± 0.063 Nm2/g respectively. Regarding wettability blend-electrospun PSI/PCL meshes exhibited the smallest contact angle (θ =109.5o ± 3.2) and shortest absorption time(t =7.55 ± 5.5 s.). Overall, PCL addition improved the mechanical performance of all the meshes both in air and under liquid while PSI once again increased wettability. (IV.)

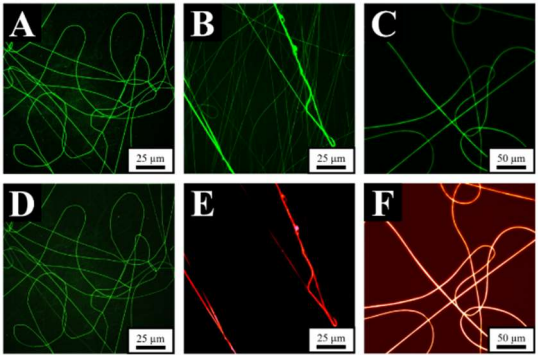

Figure 4. Fluorescent microscopy images of: A. Co-electrospun Unstained PSI/PCL - 380 nm, B. Co-electrospun stained PSI/PCL 380 nm, C Blend-spun PSI/PCL stained - 380 nm, D. Co-electrospun Unstained PSI/PCL - 480 nm, E. Co-electrospun stained PSI/PCL - 480 nm, F. Blend-electrospun stained PSI/PCL - 480 nm

T5. Biocompatibility of meshes was examined with in vitro cell and in vivo studies. Meshes proved to be cyto, haemo- and biocompatible. According to the cell studies, PSI/PCL meshes fabricated in all three setups (layer-, co-, blend-spun) are cytocompatible and exhibiting excellent cell adhesion properties. During the animal studies macroscopical and microscopical biocompatibility was evident while enhanced tissue integration after 2 weeks is highly suggestive (Figure 6,7).

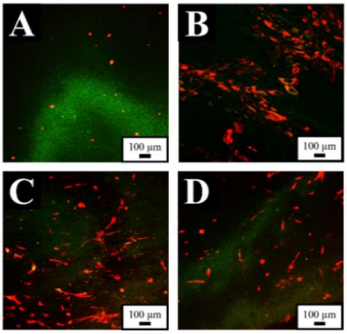

Figure 5. Two photon excitation microscopy imaging of cells placed on A. PSI-DAB, B. PCL, C. Co-spun PSI-DAB/PCL, D. Blend-spun PSI-DAB/PCL

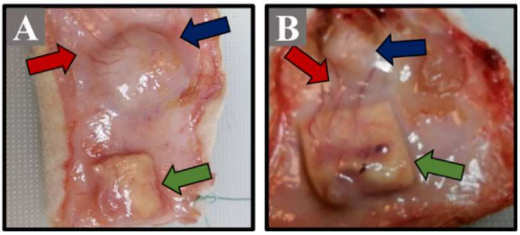

Figure 6. Macroscopical findings during sample retrieval: A. Co-spun PSI/PCL (blue arrow), Co-spun PSI-DAB/PCL (green arrow), B. Blend-spun PSI/PCL (blue arrow), Blend-spun PSI-DAB/PCL (green arrow), Newly formed vessels (neovascularisation) (red arow)

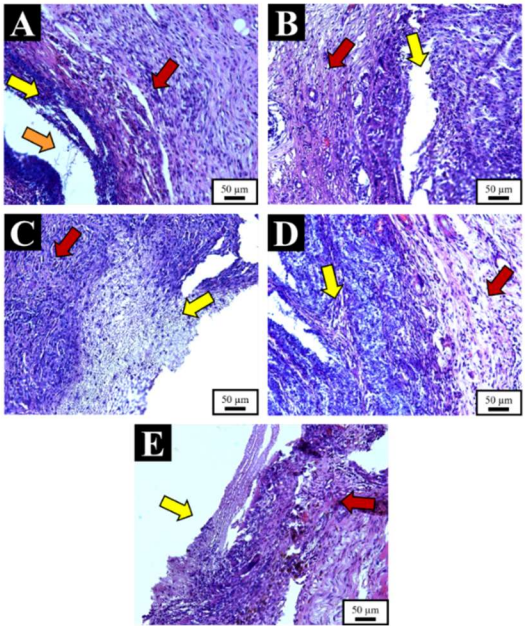

Figure 7. Histopathology examination of: A. Co-spun PSI/PCL, B. Co-spun PSI-DAB/PCL, C. Blend-spun PSI/PCL, D. Blend-spun PSI-DAB/PCL, E. PCL

T6. Incorporation of magnetite nanoparticles was successfully performed in PSI and PSI/PCL meshes. Magnetite presence was confirmed by physical (SEM, TEM) and chemical characterisation methods (ATR-FTIR). The magnetic property of the meshes was evident. Animal experiments demonstrated how PSI-DAB-Magn meshes exhibit excellent MRI contrast properties even after 8 days (Figure 8.) . Histopathology revealed no complications while magnetite diffusion was also documented in the surrounding local tissue (Figure 9.).

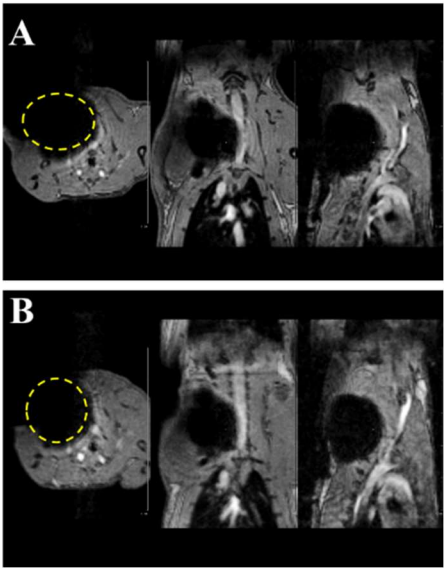

Figure 8 MRI from the 1st (A) and 8th (B) post-operative day (T2 relaxation)

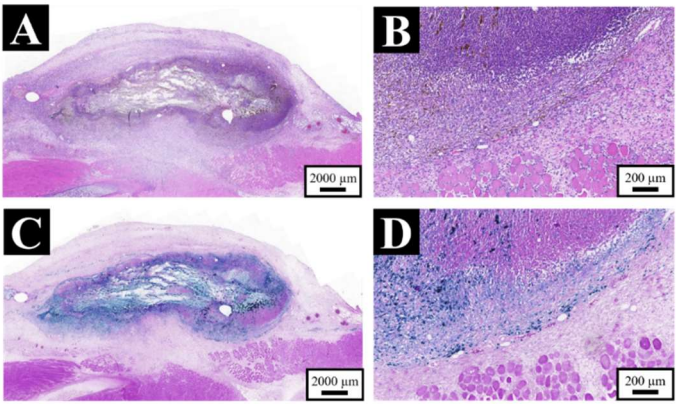

Figure 9 Sample stained with: Haematoxylin-Eosin (A, B) and Berlin Blue (C, D), Border between PSI-DAB-Magn sample, and the surrounding granulation tissue. (B) (D)

5. Conclusion

The aim of the thesis was to investigate biomaterials intended for surgical tissue regeneration. For this purpose, a promising polymer, namely polysuccinimide was investigated as well as two combinations with already utilised polymers in this field (PVA and PCL).

In the first frame of this work, PSI meshes were optimised. The average nanofibre diameter was successfully decreased to less than half the initial diameter (from 615 to 280 nm) without compromising the quality of the microstructure or the fibres. To improve the mechanical properties of these meshes, mechanically induced orientation using a rotating collector and multi-layer stacking was utilised. These methods proved successful in enhancing the uniaxial and biaxial mechanical performance of the meshes, respectively.

In the second frame PSI was co-electrospun with PVA. These meshes exhibited increased specific loading capacities under liquid, increased wettability and proved as cytocompatible and biocompatible composite meshes.

Subsequently in the third frame the PSI was combined with PCL in three different electrospinning configurations. PCL complements PSI well by increasing its overall mechanical performance (both in air and under liquid) but also providing a stable frame for cell adhesion. On the other hand, PSI increased wettability and tissue integration. The features of these composite meshes can be adjusted according to which electrospinning configuration (layer-electrospinning, co-electrospinning or blend electrospinning) is utilised. Similarly to co-spun PSI/PVA meshes, PSI/PCL meshes proved cytocompatible and biocompatible as well.

Finally, magnetite nanoparticles were incorporated with PSI meshes. The ultimate objective here will be an alternative cancer treatment option (magnetic hyperthermia) although this direction exceeds the theme of the thesis. The presence of the magnetite nanoparticles was confirmed by

physical chemical characterisation methods while meshes exhibited magnetic properties. PSI-DAB-Magn meshes were also investigated in vivo. Similarly, biocompatibility is evident even at this early stage, while more importantly the meshes proved to be an excellent MRI contrast agent. PCL was subsequently also incorporated to provide mechanical support, however its role in the functionality of this system is yet to be examined.

6. Bibliography of the candidate's publications

Publications relevant to the Thesis

I. **C. Voniatis**, L. Balsevicius, D. Barczikai, D. Juriga, A. Takács, L. Kőhidai, K. Nagy, A. Jedlovszky-Hajdu, Co-electrospun polysuccinimide/poly(vinyl alcohol) composite meshes for tissue engineering, J. Mol. Liq. 306 (2020). https://doi.org/10.1016/j.molliq.2020.112895. (Impact factor: 6.165)

II. **C. Voniatis**, D. Barczikai, G. Gyulai, A. Jedlovszky-Hajdu, Fabrication and characterisation of electrospun Polycaprolactone/Polysuccinimide composite meshes, J. Mol. Liq. 323 (2021). https://doi.org/10.1016/j.molliq.2020.115094 (Impact factor: 6.165)

III. K. Molnar, **C. Voniatis**, D. Feher, G. Szabo, R. Varga, L. Reiniger, D. Juriga, Z. Kiss, E. Krisch, G. Weber, A. Ferencz, G. Varga, M. Zrinyi, K.S. Nagy, A. Jedlovszky-Hajdu, Poly(amino acid) based fibrous membranes with tuneable in vivo biodegradation, PLoS One. 16 (2021) e0254843. https://doi.org/10.1371/journal.pone.0254843 (Impact factor: 3.240)

IV. **C. Voniatis**, R. Gottscháll, D. Barczikai, G. Szabó, A. Jedlovszky-Hajdu, Enhancing critical features of poly(amino acid) based meshes, J. Appl. Polym. Sci. 139 (2022) 51933. https://doi.org/https://doi.org/10.1002/app.51933. (Impact factor: 3.125)

V. Tamas Veres, **Constantinos Voniatis**, Kristof Molnár, Daniel Nesztor, Daniella Feher, Andrea Ferencz, Ivan Gresits, György Thuróczy, B. G. Márkus, Ferenc Simon, N. M. Nemes, M. García-Hernández, Lilla Reiniger, Ildikó Horváth, Domokos Máthé, Krisztián Szigeti, Etelka Tombácz, Angela Jedlovszky-Hajdu, An implantable magneto-responsive poly(aspartamide) based electrospun scaffold for hyperthermia treatment, Nanomaterilas, Submitted 2022 (Impact factor: 5.076)

Publications not relevant to the Thesis

1. P. Ádám, O. Temesi, Z. Dankházi, **C. Voniatis**, J. Rohonczy, K. Sinkó, Various colloid systems for drawing of aluminum oxide fibers, Ceram. Int. 48 (2022) 5499–5508. https://doi.org/https://doi.org/10.1016/j.ceramint.2021.11.094 (Impact factor: 4.527)

2. **C. Voniatis**, S. Bánsághi, A. Ferencz, T. Haidegger, A large-scale investigation of alcohol-based handrub (ABHR) volume: hand coverage correlations utilizing an innovative quantitative evaluation system, Antimicrob. Resist. Infect. Control. 10 (2021) 1–10. https://doi.org/10.1186/s13756-021-00917-8 (Impact factor: 4.887)

3. D. Fehér, A. Ferencz, G. Szabó, K. Juhos, D. Csukás, **C. Voniatis**, L. Reininger, K. Molnár, A. Jedlovszky-Hajdú, G. Wéber, Early and late effects of absorbable poly(vinyl alcohol) hernia mesh to tissue reconstruction, IET Nanobiotechnology. 15 (2021) 565–574. https://doi.org/https://doi.org/10.1049/nbt2.12015 (Impact factor: 1.847)

4. O. Hegedus, D. Juriga, E. Sipos, **C. Voniatis**, Á. Juhász, A. Idrissi, M. Zrínyi, G. Varga, A. Jedlovszky-Hajdú, K.S. Nagy, Free thiol groups on poly(aspartamide) based hydrogels facilitate tooth-derived progenitor cell proliferation and differentiation, PLoS One. 14 (2019) 1–20. https://doi.org/10.1371/journal.pone.0226363 (Impact factor: 2.740)

5. K. Molnar, **C. Voniatis**, D. Feher, G. Szabo, R. Varga, L. Reiniger, D. Juriga, Z. Kiss, E. Krisch, G. Weber, A. Ferencz, G. Varga, M. Zrinyi, K.S. Nagy, A. Jedlovszky-Hajdu, Poly(amino acid) based fibrous membranes with tuneable in vivo biodegradation, PLoS One. 16 (2021) e0254843. https://doi.org/10.1371/journal.pone.0254843 (Impact factor: 2.875)